

Transport properties of quasi-one-dimensional KRu_4O_8

W. Kobayashi*

Waseda Institute for Advanced Study, Waseda University, Tokyo 169-8050, Japan

(Received 2 December 2008; revised manuscript received 13 March 2009; published 21 April 2009)

We report resistivity, thermopower, Hall coefficient, and magnetic susceptibility of the quasi-one-dimensional (Q1D) hollandite oxide KRu_4O_8 with RuO_2 zigzag chains made of edge-shared RuO_6 octahedra. The resistivity along the chain direction (ρ_{\parallel}) is evaluated to be $1.1 \mu\Omega \text{ cm}$ at 4.2 K, which corresponds to a mean-free path along the chain direction of 2800 Å and implies that this material is one of the cleanest systems in Q1D oxides. ρ_{\parallel} is found to be proportional to $T^{2.7}$ below 62 K indicating a strong electron-electron Umklapp scattering. The temperature dependence of the thermopower is also found to derive from the expected conventional T -linear dependence and is approximately proportional to T^2 below 156 K. We discuss these peculiar transport properties using several theories for Q1D systems and also make a comparison to three-dimensional systems.

DOI: 10.1103/PhysRevB.79.155116

PACS number(s): 71.10.Pm, 72.15.-v, 72.80.Ga

I. INTRODUCTION

Quasi-one-dimensional (Q1D) materials exhibit fascinating properties such as charge density wave (CDW) in $\text{K}_{0.3}\text{MoO}_3$,¹ spin density wave (SDW) in $(\text{TMTSF})_2\text{PF}_6$,² superconductivity in Nb_3Se_4 ,³ $(\text{TMTSF})_2\text{PF}_6$,⁴ and $\beta\text{-Na}_{0.33}\text{V}_2\text{O}_5$,⁵ and charge ordering in $\text{K}_2\text{V}_8\text{O}_{16}$.⁶ In addition, ballistic conduction was recently observed in carbon nanotubes with perfect crystallinity.⁷ These Q1D materials have pairs of parallel sheetlike Fermi surfaces that are warped because of finite interchain hopping (t_{\perp}).⁸ Nesting of the Fermi surfaces causes the CDW and/or SDW states in the Q1D materials. The above properties can be explained by several theories such as one-dimensional Hubbard model, the Heisenberg model, t - J model, and the Tomonaga-Luttinger model where linear band dispersion around Fermi level is assumed. Those models commonly derive the Tomonaga-Luttinger-liquid state associated with charge-spin separation.⁹

In spite of increasing interests in the strongly correlated Q1D oxides, there have been few studies of a metallic ground state in the Q1D oxides. $\text{PrBa}_2\text{Cu}_4\text{O}_8$ is one of the most extensively studied Q1D oxides, where Narduzzo *et al.*¹⁰ recently discovered a disorder-induced one dimensionality, offering a playground between Fermi liquid and Tomonaga-Luttinger liquid. The hollandite $\text{BaRu}_6\text{O}_{12}$ (Ref. 11) is another example of Q1D oxides that exhibits metallic conduction down to 0.03 K. Mao *et al.*¹¹ proposed the existence of a quantum phase transition in this material. Recently, Foo *et al.*¹² reported the transport properties of KRu_4O_8 single crystals. They presented small resistivity of $3.5 \mu\Omega \text{ cm}$ at 0.3 K, which motivated us to study this hollandite ruthenate as a good candidate for strongly correlated Q1D oxides. We have grown single crystals of KRu_4O_8 and have measured the resistivity, thermopower, Hall coefficient, and magnetization. We find that the results are rather different from what is expected from Fermi-liquid theory. In particular, the resistivity is found not to be proportional to T^2 as expected from Fermi-liquid theory, but to $T^{2.7}$ below 62 K. Our results further suggest that the universal relation [$S/T \propto \gamma$ (Ref. 13)] between thermopower (S) and electronic

specific-heat coefficient (γ) may be modified (or violated) in the Q1D oxides. The evaluated mean-free path (l_{\parallel}) is found to be about 2800 Å, which is longer than the 215 Å found in $\text{PrBa}_2\text{Cu}_4\text{O}_8$ single crystal, which indicates that KRu_4O_8 is the cleanest Q1D system among oxides. This system should be an ideal playground to investigate novel one-dimensional properties in metallic Q1D oxides.

II. EXPERIMENTS

Single-crystal samples of KRu_4O_8 were synthesized by a self-flux method.¹² Stoichiometric amount of RuO_2 and two-time stoichiometric excess of K_2CO_3 were mixed and placed in an alumina crucible with an alumina cap. The mixture was heated at 1050 °C for 16 h and then slowly cooled down to 750 °C at a rate of -4 °C/h in N_2 flow. Needlelike crystals with a typical dimension of $1 \times 0.05 \times 0.05 \text{ mm}^3$ were grown.

X-ray diffraction of ground crystals was measured using a standard diffractometer with $\text{Cu } K_{\alpha}$ radiation as an x-ray source in the θ - 2θ scan mode. The resistivity was measured by a four-probe method, below room temperature (4.2–300 K) in a liquid He cryostat and above room temperature (300–800 K) using a home-made system with a resistive sheet heater made of RuO_2 paste in an evacuated 45 mm diameter stainless steel tube operated by a temperature controller (Neocera LTC-11). Four 20 μm gold wires were attached to the crystal with silver paste (DuPont 6838). The crystal was heated at 673 K for 10 min to harden the paste and obtain good contacts. Distances between contacts and crystal dimension were determined using a microscope with digital camera whose picture gives a precise distance.

The thermopower was measured using a steady-state technique, below room temperature (4.2–300 K) in a liquid He cryostat and above room temperature (300–800 K) in the home-made system with two platinum temperature sensors to detect small temperature gradient of about 1 K/cm. The Hall-coefficient measurement along c axis was performed using physical properties measurement system (Quantum Design) by applying 5 T. As shown in Fig. 5, four terminals made of gold wires and Ag paste are put on the crystal with a thick-

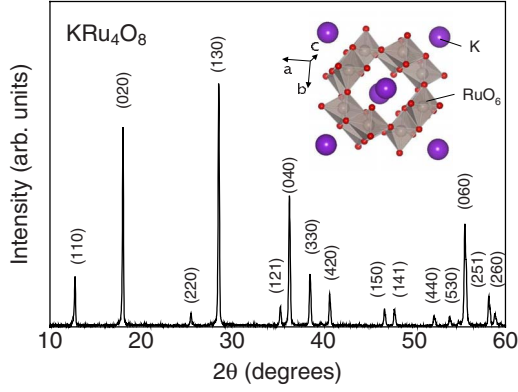


FIG. 1. (Color online) X-ray diffraction pattern of ground KRu_4O_8 crystals. Inset shows the crystal structure of KRu_4O_8 .

ness of $50 \mu\text{m}$. Typical signal of ΔV_{xy} was 0.1 mV at 5 T and was found to be linear with magnetic field. A small field-independent signal due to misalignments of the terminals was carefully subtracted by taking the antisymmetric part.

III. RESULTS AND DISCUSSION

Figure 1 shows the x-ray diffraction pattern of the ground KRu_4O_8 single crystals. All peaks were indexed to the tetragonal hollandite structure with no trace of impurity phases.¹⁴ The lattice parameters are evaluated to be $a=9.913(5) \text{ \AA}$ and $c=3.108(5) \text{ \AA}$. Q1D hollandites are denoted by $A_xB_8O_{16}$ ($A=\text{K}^+, \text{Li}^+, \text{Rb}^+, \text{Cs}^+, \text{Sr}^{2+}, \text{Ba}^{2+}, \text{and Bi}^{3+}$; $B=\text{Ti}, \text{V}, \text{Cr}, \text{Mn}, \text{Mo}, \text{Ru}, \text{Rh}, \text{and Ir}$). This crystal structure consists of BO_2 zigzag chains made of edge-shared BO_6 octahedra. The zigzag chains share corner oxygens with neighboring chains and form tunnel structures which contain A ions (see the inset of Fig. 1). The mixed-valence state between B^{3+} and B^{4+} is realized by both the valence and deficiency x of the A ion. Thus, the formal valence of the Ru ion is evaluated to be $3.75+$ in KRu_4O_8 . Depending on the width of the tunnel and the ionic radius of the A ion, the structure is found to be tetragonal or monoclinic.

Figure 2(a) shows the resistivity (ρ_{\parallel}) along the c axis of KRu_4O_8 , where metallic conduction ($d\rho_{\parallel}/dT > 0$) is observed from 4.2 to 780 K . As shown in the inset of Fig. 2, the residual resistivity is $1.1 \mu\Omega \text{ cm}$ at 4.2 K , which gives a high residual resistance ratio (RRR) of 96 [$\text{RRR} \equiv \rho_{\parallel}(300 \text{ K})/\rho_{\parallel}(4.2 \text{ K})$]. This value is larger than the RRR of 40.1 for the KRu_4O_8 crystal reported by Foo *et al.*¹² and the 2.6 – 11.3 values of the $\text{BaRu}_6\text{O}_{12}$ crystals.¹¹ We should note that the low residual resistivity is comparable to that of Sr_2RuO_4 .¹⁵ This common feature suggests good crystallinity in Ru oxides. In-chain resistivity for a one-dimensional tetragonal material with linear band dispersion along the c axis and cosine bands along a axes is described as

$$\rho_{\parallel} = \frac{\pi \hbar a^2}{e^2 l N}, \quad (1)$$

where \hbar , a , e , l , and N represent the Planck constant, the lattice parameter of the a axis, the charge unit, the mean-free path, and the number of channels in the unit cell,

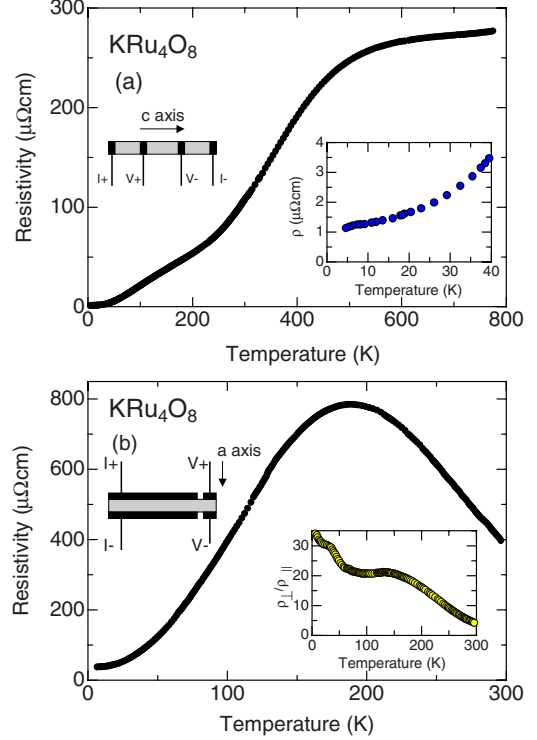


FIG. 2. (Color online) Resistivity along (a) the c axis and (b) the a axis of KRu_4O_8 . Insets of represent the resistivity at low temperatures and the anisotropy of the resistivity, respectively.

respectively.¹⁶ Using Eq. (1), l is evaluated to be $\sim 2800 \text{ \AA}$ at 4.2 K with $\rho_{\parallel}=1.1 \mu\Omega \text{ cm}$, $a=9.9 \text{ \AA}$, and $N=4$. This is equivalent to ~ 900 unit cells, being larger than ~ 60 unit cells in $\text{PrBa}_2\text{Cu}_4\text{O}_8$. As far as we know, this value is the largest reported mean-free path among Q1D oxides, which shows that KRu_4O_8 is the cleanest system. ρ_{\parallel} is found to be increase with temperature and saturates at around 500 K . ρ_{\parallel} reaches to $277 \mu\Omega \text{ cm}$ at 780 K corresponding to $l=11 \text{ \AA}$, which is rather large compared to c -axis lattice parameter of 3.1 \AA where the Mott-Ioffe-Regel limit should occur.¹⁷ Three-dimensional SrRuO_3 and two-dimensional Sr_2RuO_4 exhibit 260 and $600 \mu\Omega \text{ cm}$ at around 780 K with no indication of saturation of the resistivity showing that they are bad metals.^{18,19}

Figure 2(b) shows the temperature dependence of resistivity (ρ_{\perp}) parallel to the a axis in KRu_4O_8 . ρ_{\perp} is found to be $37.6 \mu\Omega \text{ cm}$ at 4.2 K , implying a resistivity anisotropy $\rho_{\perp}/\rho_{\parallel}$ of 34 at 4.2 K [see the inset of Fig. 2(b)], which would indicate Q1D conduction in KRu_4O_8 . This anisotropy is comparable to the value of 13 in $\text{BaRu}_6\text{O}_{12}$ (Ref. 11) and is much smaller than the $\rho_a/\rho_b \sim 1000$ in $\text{PrBa}_2\text{Cu}_4\text{O}_8$,¹⁰ indicating a weaker one dimensionality in the hollandite structure. The weak 1D feature may be related to the corner-shared RuO_2 chain networks in the ab plane. $\rho_{\perp}/\rho_{\parallel}$ increases with decreasing temperature implying that the interchain hopping t_{\perp} becomes weaker compared to the intrachain hopping t_{\parallel} , which demonstrates that the one dimensionality is reinforced at low temperatures. Similar temperature dependence of the anisotropy was reported in $\text{PrBa}_2\text{Cu}_4\text{O}_8$.²⁰ At around 72 K , ρ_{\perp} starts to deviate from the $T^{2.2}$ temperature dependence [see Fig. 3(b)] and exhibits a peak at T_{max}

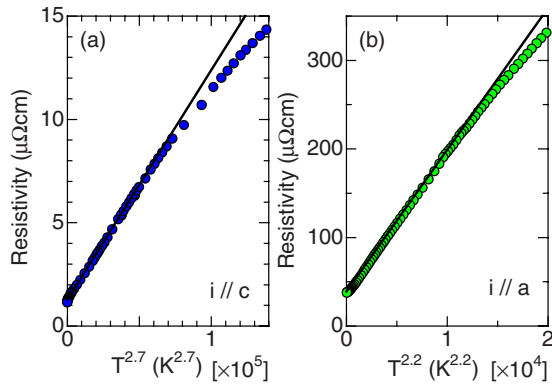


FIG. 3. (Color online) (a) ρ_{\parallel} vs $T^{2.7}$ and (b) ρ_{\perp} vs $T^{2.2}$.

=188 K. This is another characteristic for low-dimensional materials^{10,11,19,21} where semiconducting ρ_{\perp} above T_{\max} is explained by incoherent hopping due to $l \leq c'$ (l : mean-free path, c' : interlayer or interchain distance).

Below 62 K, ρ_{\parallel} is proportional to $T^{2.7}$ as shown in Fig. 3(a), which is a characteristic of Q1D conduction. A similar power is observed in Q1D TaSe₃, Nb₂Se₃, and Nb₃S₄ ($\sim T^{\alpha}$, $2 < \alpha < 3$),²² hollandite rhodium oxide Ba_{1.2}Rh₈O₁₆ ($\sim T^{2.5}$),²³ and copper oxide PrBa₂Cu₄O₈ ($\sim T^{2.3}$).¹⁰ Theoretically, the origin of the unusual power is thought to be related to the electron-electron-umklapp scattering on the material with Q1D band structure which consists of two pairs of warped sheetlike Fermi surfaces separated by about half the reciprocal-lattice vector along the chain direction.²⁴ In this case, the resistivity is proportional to T^n , where $2 \leq n \leq 3$ depending on the relative position of the two pairs of the Fermi surfaces.

Figure 4 shows magnetic susceptibility χ of collected KRU₄O₈ single crystals. χ decreases with decreasing temperature and show an upturn below 260 K corresponding to 2%-S=1/Ru. As shown in the inset of Fig. 4, M - H curve does not show any anomalies at 10 K. The temperature dependence is similar to the data previously reported by Foo *et al.*¹² They concluded that the magnetism was Pauli paramagnetism and they did not discuss the possible origins of the decrease of χ . The decrease would imply that the system tends to be nonmagnetic or antiferromagnetic. It was reported that the perovskite-type ruthenate Ba₇Li₃Ru₄O₂₀ ex-

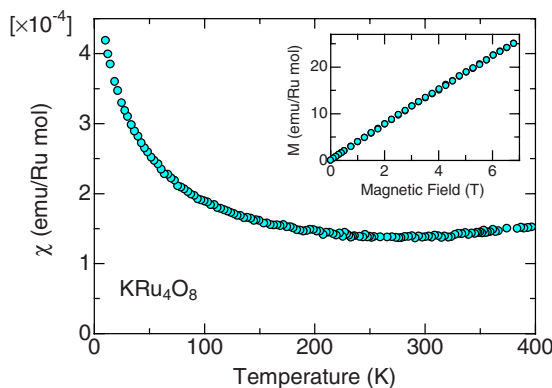


FIG. 4. (Color online) Magnetization of collected KRU₄O₈ single crystals. Inset shows M - H curve at 10 K.

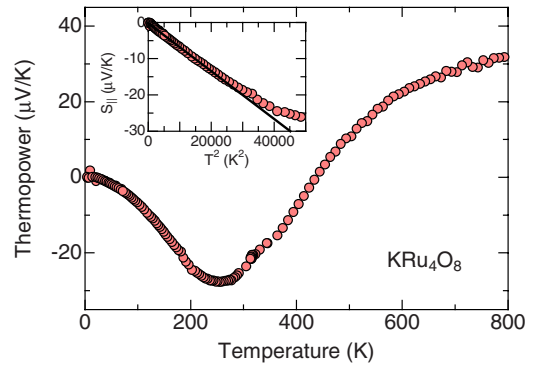


FIG. 5. (Color online) Thermopower along c axis of KRU₄O₈. Inset shows the thermopower vs T^2 below 136 K.

hibited a similar decrease of magnetization due to possible dimerization.²⁵ Narrow gap system FeSb₂ also displays a decrease of magnetization with decreasing temperature.²⁶ At high temperatures, thermally excited electrons behave as free electrons, which induces Pauli-type susceptibility at high temperatures. Pseudo-one-dimensional material α' -NaV₂O₅ also exhibits a decrease of magnetic susceptibility due to strong antiferromagnetic interaction²⁷ and this behavior is well understood by Bonner and Fisher model (one-dimensional Heisenberg model²⁸). In all three cases, conductivity is semiconducting or insulating, while KRU₄O₈ displays metallic behavior. At present, we do not know which situation is realized in KRU₄O₈ and the reason why coexistence of the metallicity and the magnetic behavior may occur.

Figure 5 shows thermopower (S_{\parallel}) along the c axis of KRU₄O₈. The temperature dependence is unusual; negative thermopower is observed below 434 K and changes sign above the temperature. At high temperatures, S_{\parallel} seems to saturate at around 32 $\mu\text{V/K}$ which is close to 33 $\mu\text{V/K}$ at 300 K seen in SrRuO₃.²⁹ The high-temperature S_{\parallel} can be explained by an extended Heikes formula³⁰ that assumes of $U \gg k_B T \gg t$ (U : on-site Coulomb repulsion energy, t : transfer energy in the one-dimensional Hubbard model, k_B : Boltzmann constant) described as

$$S = -\frac{k_B}{e} \ln \left(\frac{g_3}{g_4} \frac{x}{1-x} \right), \quad (2)$$

where g_3 , g_4 , and x represent the degeneracy of spin and orbital degree of freedom of Ru³⁺ and Ru⁴⁺ and the concentration of Ru⁴⁺ ion, respectively. Assuming low-spin states of Ru³⁺ ($S=1/2$) and Ru⁴⁺ ($S=1$), spin and orbital term ($-\frac{k_B}{e} \ln \frac{g_3}{g_4}$) yields +35 $\mu\text{V/K}$, which is consistent with our result of +32 $\mu\text{V/K}$. SrRuO₃ and Ca_{1-x}La_xRuO₃ systems were found to exhibit low-spin states [Ru⁴⁺($S=1$), Ru³⁺($S=1/2$)].^{31,32} The spin state is determined by a balance between crystal-field splitting and Hund coupling. The crystal-field splitting of RuO₆ octahedron is related to the Ru-O bond length. Since the Ru-O distances are almost the same [averaged Ru-O distance is 1.99 Å for both SrRuO₃ (Ref. 33) and KRU₄O₈ (Ref. 14)], it is reasonable to say that the spin states of Ru³⁺ and Ru⁴⁺ in KRU₄O₈ are in the low-spin states. At present, we do not know why the

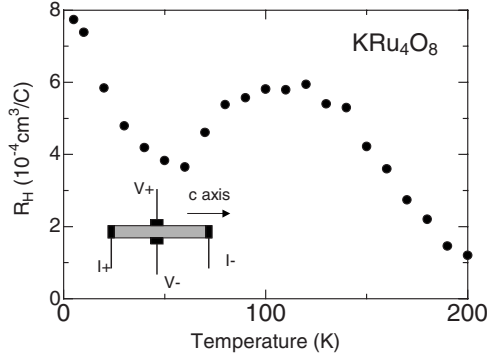


FIG. 6. Temperature dependence of Hall coefficient (R_H) of KRu_4O_8 .

thermopower is independent of carrier concentration, but similar results were observed in doped perovskite SrRuO_3 series²⁹ and several manganese oxides.³⁴

On the other hand, the temperature dependence at low temperatures is peculiar. Clearly, S_{\parallel} deviates from conventional T -linear dependence for two-dimensional (2D) and three-dimensional (3D) metals¹³ and seems to be proportional to T^2 below 156 K as shown in the inset of Fig. 5, in which neither similar results nor theories were reported. The dip of S_{\parallel} cannot also be explained by phonon drag effect which obeys T^3 temperature dependence.³⁵ According to theories for thermopower in one-dimensional materials,^{36,37} S should no longer be proportional to T at low temperatures and its temperature dependence is predicted to have a dip structure and a sign change of S at low temperatures. These theories qualitatively explain our data.

Figure 6 shows Hall coefficient (R_H) as a function of temperature in KRu_4O_8 . The temperature dependence of R_H is as complicated as $S_{\parallel}(T)$. A similar $R_H(T)$ is also observed in Q1D $\text{PrBa}_2\text{Cu}_4\text{O}_8$ where the origin is still unclear.¹⁶ However, one can analyze a high-temperature limit value of R_H . According to the theory of Hall coefficient for Q1D materials,^{38–40} R_H should saturate at high temperatures due to constant scattering time τ on the Fermi surface³⁸ and exhibits $R_H = \frac{\beta}{ne}$, where β is $\frac{2\alpha k_F}{v_F}$ ($2\alpha: \frac{\partial^2 \epsilon_k}{\partial k^2} \Big|_{k_F}$). Thus, for example, β is evaluated to be 1 for parabolic band along chain direction and $\pi/4=0.785$ for a tight-binding band 1/4 filled by holes (see Refs. 38 and 39 for the detailed calculations.) Though our data do not saturate at 200 K and we do not know the precise band dispersion; $5.2 \times 10^{22} \text{ cm}^{-3}$ is evaluated for a parabolic band model at 200 K, which is in the same order of magnitude as $2.0 \times 10^{22} \text{ cm}^{-3}$ calculated from the formal valence $\text{Ru}^{3.75+}$ in KRu_4O_8 which has eight Ru ions in the unit cell.

Lastly, we will briefly discuss the low-temperature behavior of the thermopower in Q1D oxides and compare it to the thermopower in 2D and 3D systems. Behnia *et al.*¹³ analyzed thermopower S using a single-band free-electron-gas model and found a universal relation between S/T and the electronic specific-heat coefficient γ in 2D and 3D materials. This relation implies that large γ causes large S , which can be explained with Fermi-liquid theory where strong correlation increases the effective mass. As shown in Fig. 5, S_{\parallel} of KRu_4O_8 is not proportional to T and $\text{PrBa}_2\text{Cu}_4\text{O}_8$ also exhibits $S(T)$ deviated from T -linear dependence.⁴¹ However, to check whether the universal relation works in Q1D oxides or not, we employ S/T at 4.2 K. S/T and γ are $-0.02 \mu\text{V}/\text{K}^2$ and $12 \text{ mJ}/\text{mol K}^2$ (Ref. 12) for KRu_4O_8 and $0.1 \mu\text{V}/\text{K}^2$ (Ref. 41) and $168 \text{ mJ}/\text{mol K}^2$ (Ref. 42) for $\text{PrBa}_2\text{Cu}_4\text{O}_8$, respectively. It seems that the two points significantly deviate from the universal line from Fig. 2 of Ref. 13. As discussed in their paper, this deviation may come from differences of the average carrier concentration, complicated Fermi-surface effect, and/or multiband effect. However, we would like to point out that the deviation may come from one dimensionality where the Fermi-liquid picture does not work.

IV. SUMMARY

In summary, we have shown the transport and magnetic properties of the hollandite ruthenium oxide KRu_4O_8 . The temperature dependence of resistivity ($\rho_{\parallel} \propto T^{2.7}$) indicates the existence of the electron-electron umklapp scattering between the warped sheetlike Fermi surfaces. The thermopower and the Hall coefficient are found to be semiquantitatively understood by the extended Heikes formula and the equation at high-temperature limit for one-dimensional materials, respectively. The magnitude of the resistivity is $1.1 \mu\Omega \text{ cm}$ at 4.2 K corresponding to $l_{\parallel} \sim 2800 \text{ \AA}$ and deriving large RRR of 96, which shows that this material is one of the cleanest Q1D systems in oxides.

ACKNOWLEDGMENTS

The author acknowledges I. Terasaki for fruitful discussion, M. Abdel-Jawad for critical reading of the paper, and also thanks S. Shibasaki and M. Iwakawa for technical supports. This study was partly supported by the program entitled “Promotion of Environmental Improvement for Independence of Young Researchers” under the Special Coordination Funds for Promoting Science and Technology provided by MEXT, Japan.

*kobayashi-wataru@suou.waseda.jp

¹G. Grüner, Rev. Mod. Phys. **60**, 1129 (1988).

²K. Mortensen, Y. Tomkiewicz, T. D. Schultz, and E. M. Engler, Phys. Rev. Lett. **46**, 1234 (1981).

³T. Ishida, K. Kanoda, H. Mazaki, and I. Nakada, Phys. Rev. B **29**, 1183 (1984).

⁴D. Jérôme, A. Mazaud, M. Ribault, and K. Bechgaard, J. Phys. (Paris), Lett. **41**, 95 (1980).

⁵T. Yamauchi, Y. Ueda, and N. Mori, Phys. Rev. Lett. **89**, 057002 (2002).

⁶M. Isobe, S. Koishi, N. Kouno, J. Yamaura, T. Yamauchi, H. Ueda, H. Gotou, T. Yagi, and Y. Ueda, J. Phys. Soc. Jpn. **75**,

- 073801 (2006).
- ⁷A. Bachtold, M. S. Fuhrer, S. Plyasunov, M. Forero, E. H. Anderson, A. Zettl, and P. L. McEuen, *Phys. Rev. Lett.* **84**, 6082 (2000).
- ⁸T. Giamarchi, *Chem. Rev. (Washington, D.C.)* **104**, 5037 (2004).
- ⁹For example, H. J. Schulz, arXiv:cond-mat/9503150 (unpublished).
- ¹⁰A. Narduzzo, A. Enayati-Rad, P. J. Heard, S. L. Kearns, S. Horii, F. F. Balakirev, and N. E. Hussey, *New J. Phys.* **8**, 172 (2006).
- ¹¹Z. Q. Mao, T. He, M. M. Rosario, K. D. Nelson, D. Okuno, B. Ueland, I. G. Deac, P. Schiffer, Y. Liu, and R. J. Cava, *Phys. Rev. Lett.* **90**, 186601 (2003).
- ¹²M. L. Foo, Wei-Li Lee, T. Siegrist, G. Lawes, A. P. Ramirez, N. P. Ong, R. J. Cava, *Mater. Res. Bull.* **39**, 1663 (2004).
- ¹³K. Behnia, D. Jaccard, and J. Flouquet, *J. Phys.: Condens. Matter* **16**, 5187 (2004).
- ¹⁴M. Wilhelm and R. Hoppe, *Z. Anorg. Allg. Chem.* **438**, 90 (1978).
- ¹⁵N. Kikugawa and Y. Maeno, *Phys. Rev. Lett.* **89**, 117001 (2002).
- ¹⁶S. Horii, H. Takagi, H. Ikuta, N. E. Hussey, I. Hirabayashi, and U. Mizutani, *Phys. Rev. B* **66**, 054530 (2002).
- ¹⁷N. F. Mott, *Metal-Insulator Transition*, 2nd ed. (Taylor & Francis, London, 1990).
- ¹⁸P. B. Allen, H. Berger, O. Chauvet, L. Forro, T. Jarlborg, A. Junod, B. Revaz, and G. Santi, *Phys. Rev. B* **53**, 4393 (1996).
- ¹⁹A. W. Tyler, A. P. Mackenzie, S. Nishizaki, and Y. Maeno, *Phys. Rev. B* **58**, R10107 (1998).
- ²⁰S. Horii, U. Mizutani, H. Ikuta, Y. Yamada, J. H. Ye, A. Matsushita, N. E. Hussey, H. Takagi, and I. Hirabayashi, *Phys. Rev. B* **61**, 6327 (2000).
- ²¹I. Terasaki, Y. Sasago, and K. Uchinokura, *Phys. Rev. B* **56**, R12685 (1997).
- ²²M. H. Rashid and D. J. Sellmyer, *Phys. Rev. B* **29**, 2359 (1984).
- ²³W. Kobayashi, S. Hebert, O. Perez, D. Pelloquin, and A. Maignan, *Phys. Rev. B* **79**, 085207 (2009).
- ²⁴A. Oshiyama, K. Nakao, and H. Kamimura, *J. Phys. Soc. Jpn.* **45**, 1136 (1978).
- ²⁵K. E. Stitzer, W. R. Gemmill, M. D. Smith, and H.-C. zur Loye, *J. Solid State Chem.* **175**, 39 (2003).
- ²⁶T. Koyama, Y. Fukui, Y. Muro, T. Nagao, H. Nakamura, and T. Kohara, *Phys. Rev. B* **76**, 073203 (2007).
- ²⁷M. Isobe and Y. Ueda, *J. Phys. Soc. Jpn.* **65**, 1178 (1996).
- ²⁸W. E. Hatfield, *J. Appl. Phys.* **52**, 1985 (1981).
- ²⁹Y. Klein, S. Hébert, A. Maignan, S. Kolesnik, T. Maxwell, and B. Dabrowski, *Phys. Rev. B* **73**, 052412 (2006).
- ³⁰W. Koshibae, K. Tsutsui, and S. Maekawa, *Phys. Rev. B* **62**, 6869 (2000).
- ³¹H.-T. Jeng, S.-H. Lin, and C.-S. Hsue, *Phys. Rev. Lett.* **97**, 067002 (2006).
- ³²T. Sugiyama and N. Tsuda, *J. Phys. Soc. Jpn.* **68**, 3980 (1999).
- ³³M. Shikano, Tong-Kai Huang, Y. Inaguma, M. Itoh, and T. Nakamura, *Solid State Commun.* **90**, 115 (1994).
- ³⁴W. Kobayashi, I. Terasaki, M. Mikami, R. Funahashi, T. Nomura, and T. Katsufuji, *J. Appl. Phys.* **95**, 6825 (2004).
- ³⁵J. M. Ziman, *Principles of the Theory of Solids* (Cambridge University Press, Cambridge, England, 1979).
- ³⁶M. M. Zempljic and P. Prelovsek, *Phys. Rev. B* **71**, 085110 (2005).
- ³⁷M. R. Peterson, S. Mukerjee, B. S. Shastry, and J. O. Haerter, *Phys. Rev. B* **76**, 125110 (2007).
- ³⁸V. M. Yakovenko and A. T. Zheleznyak, *Synth. Met.* **103**, 2202 (1999).
- ³⁹A. Lopatin, A. Georges, and T. Giamarchi, *Phys. Rev. B* **63**, 075109 (2001).
- ⁴⁰G. Léon, C. Berthod, and T. Giamarchi, *Phys. Rev. B* **75**, 195123 (2007).
- ⁴¹I. Terasaki, N. Seiji, S. Adachi, and H. Yamauchi, *Phys. Rev. B* **54**, 11993 (1996).
- ⁴²H. D. Yang, J.-Y. Lin, S. S. Weng, C. W. Lin, H. L. Tsay, Y. C. Chen, T. H. Meen, T. I. Hsu, and H. C. Ku, *Phys. Rev. B* **56**, 14180 (1997).